

## **Treated and untreated anovulation associated with ovarian and uterine blood flow in Arabian mares (a case study)**

**Amal M. Abo El-Maaty<sup>1#</sup>, Yehia El Baghdady<sup>2</sup>, Khalid A. ElShahat<sup>2</sup>, Mahmoud A. Helmy<sup>2</sup>, Elshymaa A. Abdelnaby<sup>2</sup>**

<sup>1</sup>National Research Center, Veterinary Division, Animal Reproduction and AI Department, Dokki, Egypt; #e-mail: amalaboelmaaty1@yahoo.com

<sup>2</sup>Cairo University, Faculty of Veterinary Medicine, Theriogenology Department, Egypt

To investigate the development of treated and untreated hormonal anovulatory follicles (AnOV) associated with uterine and ovarian vascularization, rectal Doppler ultrasound of seven Arabian mares was performed before and after the development of an AnOV. In addition to measuring the diameter, area and volume of the follicle, daily colour and power Doppler scans were analysed in order to measure red, blue and power blood flow areas in pixels. Serum levels of estradiol (E2), progesterone (P4), leptin, insulin-like growth factor-I (IGF-1) and nitric oxide (NO) were measured as well. The diameter (cm), area (cm<sup>2</sup>), volume (cm<sup>3</sup>), area in pixels, antral area in pixels, circumference, and percentage change in circulation of the AnOV progressively increased ( $P<0.0001$ ) after the disappearance of uterine oedema compared to the values obtained during oedema. The blue, total colour and power areas of the AnOV increased after the disappearance of uterine oedema ( $P<0.0001$ ). When the antral area was excluded, the percentage of the granulosa layer in the colour and power Doppler decreased after the disappearance of uterine oedema. The ipsilateral uterine horn and uterine body had significantly ( $P<0.0001$ ) high blue and red blood flow vascularization areas in the presence of uterine oedema. The AnOV was associated with low P4, IGF-1 ( $P<0.001$ ), and leptin ( $P<0.05$ ). Treatment of the AnOV follicle with GnRH resulted in its luteinization and induced ovulation 9 and 30 days later. It can be concluded that an abrupt increase in blood flow due to decreased progesterone and E2 and increased IGF-1 causes anovulation. The absence of oestrous behaviour and high uterine-oedema-associated follicular and ipsilateral uterine horn vascularization are predictors of ovulation failure.

**KEY WORDS:** anovulation / colour Doppler / power Doppler / uterine blood flow / hormones / mare

In the last two decades, Doppler technology has been extensively used in reproductive diagnostics to examine ovarian [2, 3, 4, 5, 6, 12, 15, 16, 17, 18, 24, 36, 38], and uterine [1, 8, 9, 13, 14, 22, 23, 25, 26, 32, 39] blood flow in mares.

In mares, the incidence of failure of ovulation of the dominant follicle near the end of oestrus has been shown to be low (5%) in comparison to both the autumn transition period (20%) [34] and the period preceding the ovulatory wave (25%) [30]. The number of mares developing dominant anovulatory follicles during the transitional period varies among reports, e.g. 15 of 15 [43], nine of ten [20], or three of eight [21]. The development of a dominant follicle, whether anovulatory or ovulatory, is associated with a follicular wave and a deviation process wherein the developing dominant follicle continues to grow, and alternate subordinate follicles undergo atresia [31]. The attributes of deviation are comparable for occasional anovulatory follicular waves with dominant follicles and seasonal ovulatory waves [7].

This study aimed to investigate the changes in AnOV dimensions and blood flow associated with peripheral blood hormone levels and uterine blood flow in the case of an anovulatory follicle in Arabian mares, in the presence of uterine oedema and after its disappearance.

## Materials and Methods

*Animals and ultrasound scanning.* The animals used in the study were healthy, adult, cycling Egyptian Arab mares ( $n = 7$ ) belonging to the Ministry of the Interior (30.0276°N, 31.2101°E), aged 4–11 years and weighing  $320 \pm 30$  kg. Feeding and housing conditions were uniform for all mares. They were kept individually in an indoor paddock under natural light and temperature with artificial lighting at night. They were fed a commercial concentrated feed ration and hay with clean water.

One mare was subjected to daily Doppler ultrasound examination (SonoAceR3, Medison, Samsung, South Korea) (Figure 1A-C). The others were diagnosed and treated (Figure 1 D-L) until two consecutive ovulations had been diagnosed, with the day of treatment designated as day 0. The study was performed in accordance with the guidelines of the Institutional Animal Care and Use Committee (IACUC) of the Faculty of Science, Cairo University, and the National Research Centre. Blood flow vascularization (Figure 1) area was determined as previously described for ovarian follicles [3, 4], uterine horns, and uterus [23]. Blood flow was measured by colour and power Doppler only in the case of the largest ovarian follicle associated with uterine oedema (Days 1-5), after uterine oedema (days 6 to 10), and on days 11 to 17. The total coloured area is the sum of the blue and red areas in pixels. The coloured area % is the ratio of the total coloured area in pixels to the follicle area in pixels. The granulosa coloured area % is the ratio of the coloured area to the follicle area minus

the antral area. The power area % is the ratio of the power area in pixels to the follicle area. The granulosa power area % is the ratio of the power area to the follicle area minus the antral area.

*Blood sampling and hormone assays.* Daily blood samples were collected from all mares via jugular vein punctures into plain vacuum tubes. Serum was harvested and stored at  $-20^{\circ}\text{C}$  until hormone determination. Sensitivity of the assay to progesterone (P4, EIA-1561) was 0.045 ng/mL and the intra- and inter-precision were 5.4 and 9.96, respectively. The estradiol (E2 EIA-2693) sensitivity of the assay is 9.714 pg/mL, and test intra- and inter-precisions are 6.81 and 7.25. In the Leptin Sandwich assay (EIA-2395), the lower limit of detection was 1.0 ng/mL, with intra-assay and inter-assay coefficients of variation of 3.1% and 9.7%. The sensitivity of the insulin-like growth factor-I assay (IGF-1 600, EIA-4140) was 1.29 ng/mL, with intra- and inter-precisions of 6.62 and 7.79. All the hormones were assayed using commercial ELISA kits (DRG, International Inc., USA). To measure nitric oxide metabolites (NO), serum samples were mixed with an equal volume of freshly prepared Griess reagent and incubated for 10 minutes at room temperature; absorbance was measured at 540 nm using a microtitre plate reader. Nitrite ( $\text{NO}_2$ ) standards (0–50 mM) were used to determine NOM concentrations in each well as in the previous measurements in our laboratory in mares [3, 4]. The intra- and inter-assay coefficients of variation for the NOM assay were 5.3% and 6.9%, respectively. The sensitivity of the assay was 0.225 mmol/L.

*Image analysis.* The blood flow area in the follicle wall, uterine horns and uterine body was measured in pixels, as previously described in cows [7] and mares [3, 4, 23], using Adobe PhotoShop CC software (1990-2013, Adobe Systems).

*Statistical analysis.* Data are presented as Mean  $\pm$ SEM (standard error of mean) using SPSS software [40]. Simple one-way ANOVA was used to test the effect of the phase of the oestrous cycle on the follicle diameter (cm), area ( $\text{cm}^2$ ), volume ( $\text{cm}^3$ ), area in pixels, follicle antrum area in pixels, area of granulosa layer in pixels, blue and red areas in pixels, power area in pixels, colour and power area percentages of the follicle and granulosa layer in pixels, and blue, red and power areas in pixels of the ipsilateral and contralateral uterine horns and uterine body. Duncan's Multiple Range Test was performed to compare significant differences between means at  $P < 0.05$ .

## Results and discussion

The diameter (cm), area ( $\text{cm}^2$ ), volume ( $\text{cm}^3$ ), area in pixels, antral area in pixels, circumference, and circulation % of the AnOV (Table 1, Figure 2) increased ( $P < 0.0001$ ) progressively after the disappearance of uterine oedema compared to the values during oedema. The blue, total colour and power areas of the AnOV increased

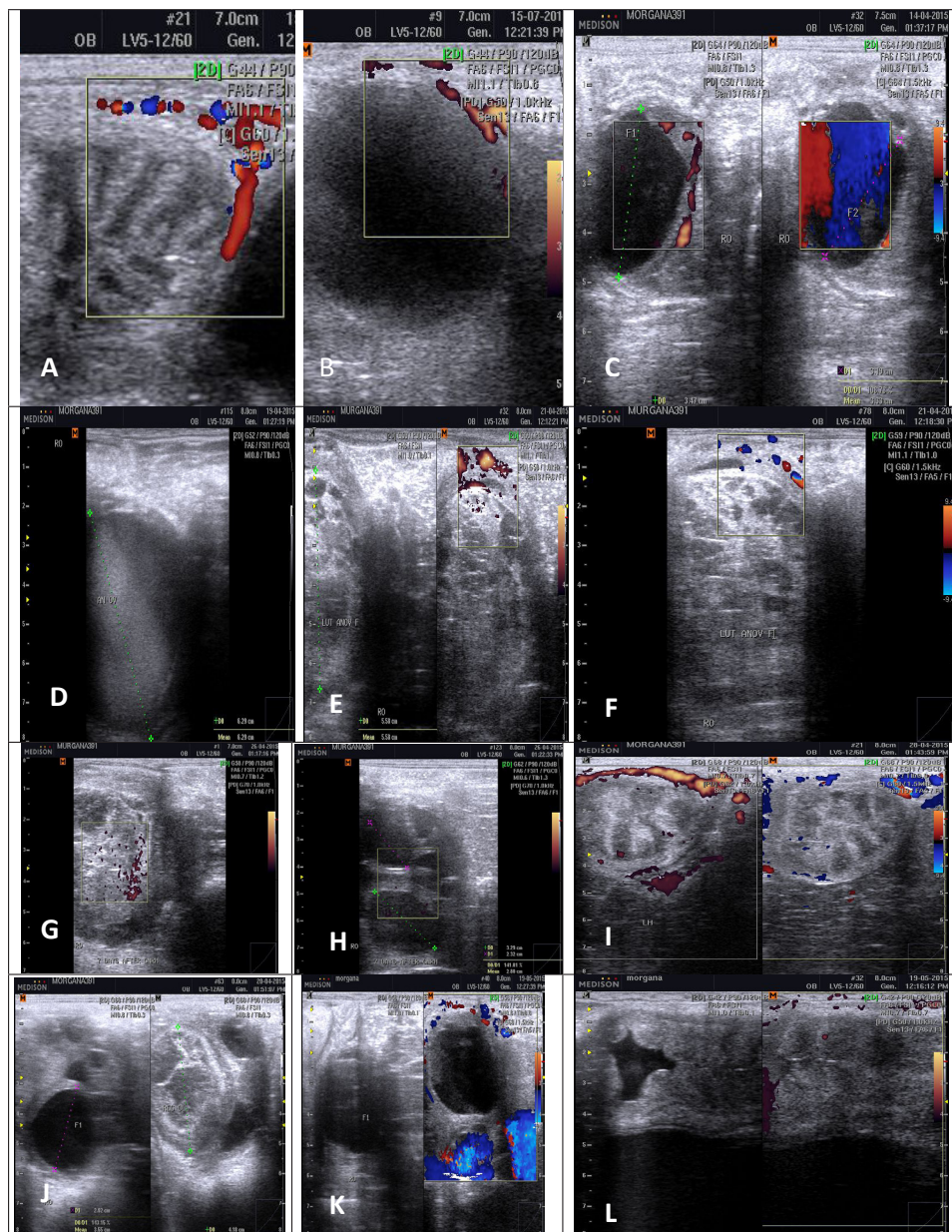


Fig. 1. Ultrasonogram of uterine oedema: A – with colour Doppler during development of untreated AnOV follicle, B – with power Doppler. C – AnOV with colour (right) and power (left) Doppler 5 days before anovulation. D – day 0 – AnOV with diameter >60 mm treated with GnRH. E – day 2 after GnRH with power and F – colour Doppler. G – day 7 after GnRH with power and H – next

ovulatory wave. I – day 9 after uterine oedema with power (left) and colour (right) Doppler. J – next ovulating follicle 31 mm in diameter (left) and regressing luteinized AnOV 41 mm in diameter (right). K – day 30 after GnRH second ovulating follicle of 35mm with colour Doppler and L – uterine body after breeding with power Doppler

after the disappearance of uterine oedema ( $P<0.0001$ ). The total colour and power area of the AnOV decreased ( $P<0.0001$ ) after disappearance of uterine oedema and after 13 days. When the antrum area was excluded, the percentage of granulosa colour and power area decreased ( $P<0.0001$ ) after the disappearance of uterine oedema. The ipsilateral uterine horn and uterine body had significantly ( $P<0.0001$ ) larger blue and red blood flow vascularization areas during uterine oedema. The AnOV was associated with low progesterone (P4) from days 1–5 and days 5–10, compared to days 11–18, when another dominant follicle developed. IGF-1 ( $P<0.001$ ) and leptin ( $P<0.05$ ) decreased after the disappearance of uterine oedema.

The progesterone concentrations were positively correlated (Table 2) with AnOV diameter ( $r=0.55$ ;  $P<0.01$ ), area ( $r=0.78$ ;  $P<0.0001$ ), and antrum area ( $r=0.78$ ;  $P<0.0001$ ), and negatively with the blue area ( $r=-0.72$ ;  $P<0.0001$ ), power area and granulosa power area % ( $r=-0.52$ ;  $P<0.0001$ ), total colour area and granulosa colour area % ( $r=-0.73$ ;  $P<0.0001$ ), total colour area % ( $r=-0.71$ ;  $P<0.0001$ ), granulosa power area ( $r=-0.59$ ;  $P<0.0001$ ), and the ipsilateral uterine horn blue ( $r=-0.71$ ;  $P<0.0001$ ), red, and power areas ( $r=-0.57$ ;  $P<0.0001$ ).

Estradiol (E2) was equally positively correlated (Table 2) with the blue blood flow area, total colour area, and total granulosa colour area % ( $r=0.37$ ;  $P<0.01$ ), but negatively with the red blood flow area ( $r=-0.37$ ;  $P<0.01$ ).

IGF-1 correlated negatively with the AnOV diameter ( $r=-0.46$ ;  $P<0.01$ ), but positively with the blue ( $r=0.35$ ;  $P<0.05$ ) and power area and the granulosa power area % ( $r=0.44$ ;  $P<0.01$ ), the total colour area and granulosa colour area % ( $r=0.36$ ;  $P<0.05$ ), the total colour area % ( $r=0.38$ ;  $P<0.05$ ), and the granulosa power area ( $r=0.45$ ;  $P<0.01$ ). Leptin had negative correlations with diameter, area and antral area, but positive correlations with all AnOVs, the blue granulosa layer, and power vascularization (Table 2).

This study reported a spontaneous untreated anovulatory follicle among 15 ovulatory follicles and another case of a treated AnOV among 13 ovulating follicles. According to our previous findings, the incidence of haemorrhagic anovulatory follicles (HAFs) ranges from 5% to 20% of oestrous cycles during the early and late ovulatory season [33], and their development has been associated with low concentrations of anti-Müllerian hormone in mares [29]. The untreated mare with spontaneous AnOV in the current study was young, aged 4–5 years, while the treated one was <20 years.

**Table 1**

Dimensions of an AnOV follicle, vascularization of the follicle and uterus in colour and power Doppler, and hormonal changes during the development of an untreated AnOV follicle

Item	Days 1-5 during uterine oedema	Days 6-10 after uterine oedema	Days 11-18 after uterine oedema	P-value
1	2	3	4	5
Diameter (cm)	3.40 <sup>a</sup> ±0.04	4.03 <sup>b</sup> ±0.06	4.23 <sup>c</sup> ±0.04	<0.0001
Area (cm <sup>2</sup> )	10.93 <sup>a</sup> ±0.33	15.56 <sup>b</sup> ±0.40	17.00 <sup>c</sup> ±0.33	<0.0001
Volume (cm <sup>3</sup> )	17.51 <sup>a</sup> ±0.68	30.98 <sup>b</sup> ±1.17	35.30 <sup>c</sup> ±0.99	<0.0001
Area (pixels)	67 195 <sup>a</sup> ±1531	98 301 <sup>b</sup> ±7379	132 257 <sup>c</sup> ±1645	<0.0001
Antrum area (pixels)	60 674 <sup>a</sup> ±1531	91 780 <sup>b</sup> ±7380	125 736 <sup>c</sup> ±1645	<0.0001
Granulosa area	6521 ±10,51	6521 ±0.01	6521 ±0,01	=0.40
Circumference	913 <sup>a</sup> ±19	1211 <sup>b</sup> ±59	1452 <sup>c</sup> ±34	<0.0001
Circulation (%)	73.40 <sup>a</sup> ±0.62	76.15 <sup>b</sup> ±0.32	80.00 <sup>c</sup> ±0.47	<0.0001
Blue blood flow area	4257 <sup>c</sup> ±77	2589 <sup>b</sup> ±256	1607 <sup>a</sup> ±128	<0.0001
Red blood flow area	1492 <sup>a</sup> ±32	1629 <sup>b</sup> ±29	1696 <sup>b</sup> ±14	<0.0001
Total coloured area	5749 <sup>c</sup> ±50	4218 <sup>b</sup> ±228	3304 <sup>a</sup> ±115	<0.0001
Power blood flow area	5706 <sup>c</sup> ±158	2839 <sup>b</sup> ±145	2464 <sup>a</sup> ±26	<0.0001
Coloured area (%)	8.59 <sup>c</sup> ±0.15	4.73 <sup>b</sup> ±0.49	2.51 <sup>a</sup> ±0.12	<0.0001
Coloured granulosa area (%)	88.16 <sup>c</sup> ±0.76	64.7 <sup>b</sup> ±3.49	50.7 <sup>a</sup> ±1.76	<0.0001
Power area (%)	8.49 <sup>c</sup> ±0.12	3.18 <sup>b</sup> ±0.33	1.87 <sup>a</sup> ±0.04	<0.0001
Power granulosa area (%)	87.51 <sup>c</sup> ±2.42	43.53 <sup>b</sup> ±2.23	37.8 <sup>a</sup> ±0.39	<0.0001
Blue ipsilateral horn area	2407 <sup>c</sup> ±32	2185 <sup>b</sup> ±121	1929 <sup>a</sup> ±36	<0.0001

<b>1</b>	<b>2</b>	<b>3</b>	<b>4</b>	<b>5</b>
Red ipsilateral horn area	1453 <sup>b</sup> ±22	1251 <sup>a</sup> ±53	1205 <sup>a</sup> ±15	<0.0001
Power ipsilateral horn area	3292 <sup>c</sup> ±97	2597 <sup>b</sup> ±75	2414 <sup>a</sup> ±23	<0.0001
Blue contralateral horn area	1070 <sup>a</sup> ±45	1332 <sup>b</sup> ±113	1559 <sup>c</sup> ±38	<0.0001
Red contralateral horn	981 <sup>c</sup> ±15	835 <sup>b</sup> ±58	698 <sup>a</sup> ±11	<0.0001
Power contralateral horn area	2203 <sup>a</sup> ±100	2269 <sup>ab</sup> ±65	2393 <sup>b</sup> ±28	=0.025
Blue uterine body area	4715 <sup>b</sup> ±36	4511 <sup>b</sup> ±218	3916 <sup>a</sup> ±38	=0.001
Red uterine body area	1229 <sup>b</sup> ±25	1042 <sup>a</sup> ±29	1011 <sup>a</sup> ±9.59	<0.0001
Power uterine body area	3457 <sup>a</sup> ±11	3554 <sup>b</sup> ±57	3641 <sup>b</sup> ±21	<0.0001
P4 (ng/ml)	1.18 <sup>a</sup> ±0.14	1.36 <sup>a</sup> ±0.24	3.35 <sup>b</sup> ±0.25	<0.0001
E2 (pg/ml)	180 ±4.3	169 ±8.4	169 ±9.5	=0.593
IGF-1 (ng/ml)	269 <sup>b</sup> ±11.3	227 <sup>a</sup> ±7.9	227 <sup>a</sup> ±5.8	=0.001
Leptin (ng/ml)	1.40 <sup>b</sup> ±0.09	1.23 <sup>a</sup> ±0.03	1.19 <sup>a</sup> ±0.03	=0.026
NO (µmol/l)	32.59 ±2.86	30.69 ±2.23	30.62 ±1.66	=0.26

Means with different superscripts (a, b, c) within rows are significant at P<0.05

However, anovulation is more common in mares older than 20 years, tends to recur in individuals, and is most common during the late follicular phase [41]. Although the non-treated anovulatory follicle did not become haemorrhagic for 12 days after disappearance of uterine oedema, it had a higher maximum diameter than the average ovulatory follicle diameter in Arabian mares [3]. The treated AnOV follicle was detected five days after predicted ovulation, and its diameter exceeded 60 mm. In agreement with our results, some anovulatory follicles achieve a size that is indistinguishable from the most extreme width of an ovulatory follicle [33, 43]. The natural occurrence of a spontaneous luteinized anovulatory follicle is difficult to predict [19]. In contrast with the increased power, blue and red blood flow area before the occurrence of the

**Table 2**

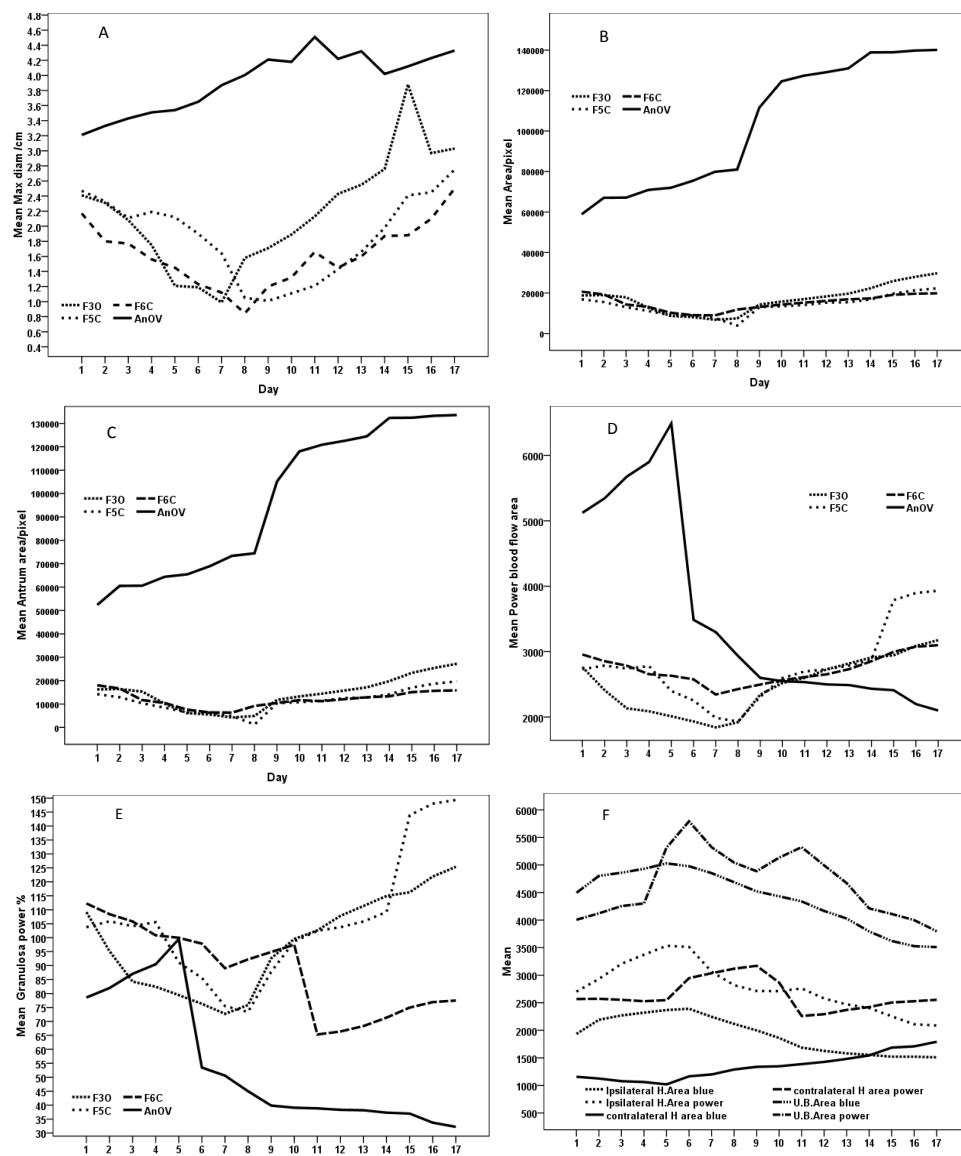
Pearson correlation coefficients among circulating hormones, follicle dimensions, blood flow and ipsilateral uterine horn blood flow during AnOV development

Item	E2 (pg/ml)	P4 (ng/ml)	Leptin (ng/ml)	IGF-1 (ng/ml)
Max diameter (cm)	-0.13 <sup>+</sup>	0.55 <sup>**</sup>	-0.62 <sup>**</sup>	-0.46 <sup>**</sup>
Area (pixels)	-0.32 <sup>+</sup>	0.78 <sup>***</sup>	-0.52 <sup>*</sup>	-0.32 <sup>+</sup>
Antrum area (pixels)	-0.32 <sup>+</sup>	0.78 <sup>***</sup>	-0.89 <sup>***</sup>	-0.32 <sup>+</sup>
Blue blood flow area	0.37 <sup>*</sup>	-0.72 <sup>***</sup>	0.89 <sup>***</sup>	0.35 <sup>*</sup>
Red blood flow area	-0.37 <sup>*</sup>	0.61 <sup>***</sup>	-0.88 <sup>***</sup>	-0.22 <sup>+</sup>
Power blood flow area (pixels)	0.21 <sup>+</sup>	-0.52 <sup>**</sup>	0.63 <sup>**</sup>	0.44 <sup>**</sup>
Total coloured area	0.37 <sup>*</sup>	-0.73 <sup>**</sup>	0.88 <sup>***</sup>	0.36 <sup>*</sup>
Total coloured area (%)	0.29 <sup>+</sup>	-0.71 <sup>***</sup>	0.81 <sup>***</sup>	0.38 <sup>*</sup>
Coloured granulosa area (%)	0.37 <sup>*</sup>	-0.73 <sup>***</sup>	0.88 <sup>***</sup>	0.36 <sup>*</sup>
Power granulosa area	0.22 <sup>+</sup>	-0.59 <sup>***</sup>	0.67 <sup>**</sup>	0.45 <sup>**</sup>
Power granulosa area (%)	0.21 <sup>+</sup>	-0.52 <sup>**</sup>	0.63 <sup>***</sup>	0.44 <sup>**</sup>
Blue ipsilateral horn area	0.39 <sup>*</sup>	-0.71 <sup>***</sup>	0.97 <sup>***</sup>	0.13 <sup>+</sup>
Red ipsilateral horn area	0.33 <sup>*</sup>	-0.57 <sup>***</sup>	0.86 <sup>***</sup>	0.35 <sup>*</sup>
Power ipsilateral horn area	0.26 <sup>+</sup>	-0.57 <sup>***</sup>	0.70 <sup>**</sup>	0.46 <sup>**</sup>

<sup>+</sup>means P>0.05; <sup>\*</sup>means P<0.05, <sup>\*\*</sup>means P<0.01, <sup>\*\*\*</sup>means P<0.0001

AnOV in the presence of uterine oedema, when both the ovulatory and anovulatory follicle were 25 to 30 mm in diameter, the blood flow area was small in the anovulatory follicle compared to the ovulatory follicle [16]. Although the power blood flow vascularization area of the AnOV appeared to be the largest in comparison with subsequent growing dominant and subordinate follicles (Figure 1C), when the granulosa power Doppler vascularization percentage was counted, it proved to be the smallest





F30 – follicle on the ovulating ovary, F5C and F6C – follicles on the contralateral ovary (A-E)

Fig. 2. Means: diameter (A), area in pixels (B), antrum area (C), power blood flow vascularization (D), granulosa power area % of growing follicles associated with the AnOV (E), blue and power vascularization of uterine horns and uterine body (F)

(Figure 1D). Similarly, the mean blood flow area was two times greater for the 30 mm ovulatory follicles than for anovulatory follicles of the same diameter [33].

Compared to the ovulatory follicles [3, 4], the AnOV had a similar diameter from day 1 to day 5, after which its diameter, area and blood flow area progressively increased after the disappearance of uterine oedema (Day 5). Similarly, the dominant anovulatory follicles 30 mm in diameter had a smaller diameter with lower blood flow area than the ovulatory follicles on each day beginning on day 1, when the follicles were 25 mm or greater [16]. The reduced blue and power vascularity, coloured area %, and coloured granulosa area % could be associated with reduced proliferation of endothelial cells in follicle capillaries and reduced theca vascularity [37]. Similar to the high percentage of AnOV wall (granulosa area) in the colour ( $88.16 \pm 0.76$ ) and power ( $87.51 \pm 2.42$ ) Doppler signals from day 1 to day 5, a higher percentage of follicle wall with colour Doppler ( $90\% \pm 4\%$ ) has been observed in a group of haemorrhagic anovulatory follicles (HAF) [33]. This increase in the percentage of follicle wall in the colour and power Doppler was attributable to vascularization of the follicle wall in the area of expected ovulation (apical area) in mares with an HAF, but not in mares that ovulated with different follicle diameters [33].

The decrease in progesterone to below 2 ng/ml for five successive days before transformation of the follicle into an AnOV and 5 days after transformation into an AnOV indicates the role of this hormone in the maturation and ovulation of the dominant follicle, which was clearly observed when P4 increased to above 3 ng/mL during the development of the next dominant follicle. This progesterone may be produced by luteinization of the AnOV after the diameter increases and the follicle is filled with echogenic particles, or by the next dominant or subordinate granulosa cells, in order to avoid a second anovulation [33, 41]. The decreasing blood flow in the AnOV was significantly correlated with a decrease in leptin. In contrast, in the preovulatory follicle, nutritional deficiencies due to short-term feed restriction are compensated for by an increase in vascularization, through a decrease in both systemic and intrafollicular leptin concentrations [28]. The significantly decreased systemic concentrations of IGF-1, E2 and leptin when uterine oedema diminished in the mare with the AnOV might be the cause of anovulation, since intrafollicular IGF-1 decreased and was associated with high E2 in mares during the final stages of follicular growth above 40 mm, as well as those with impending ovulation [11]. The significant positive correlations of IGF-1 with all cases of AnOV power and blue vascularization are indicative of the role of this hormone in regulating follicle function and ovulation. In granulosa cells of mature follicles, IGF-1, together with gonadotropins, promotes hormone secretion and follicular growth and prevents apoptosis. Similarly, preovulatory follicle blood flow has been correlated with plasma concentrations of IGF-1 and E2 in buffaloes [42]

and mares [35]. The decreased systemic E2 in the case of AnOV could result from decreased follicular meiosis activating sterols (MAS), which play a physiological role during preovulatory maturation [10]. The decrease in the area of the granulosa layer, proliferation-associated decrease in E2 and P4 concentrations, and anovulation could be associated with decreased concentrations of vascular endothelial growth factor (VEGF), which is essential for normal follicular angiogenesis and function [27].

This study concluded that the anovulatory follicle attains a maximum diameter higher than that of an ovulatory one, with a high antral area and apparent vascular perfusion during the follicular growth phase, as well as a small blue and power blood flow area after the disappearance of oestrus signs and uterine oedema. Anovulatory follicles vary in terms of vascular perfusion, which helps in selecting follicles for assisted reproductive techniques.

*Acknowledgements.* The authors wish to thank the veterinary officers of the Ministry of the Interior of Egypt for consenting to Doppler examination and blood sampling of horses for this study and the National Research Centre in Egypt for providing the Doppler scanner.

#### REFERENCES

1. ABDELNABY E.A., ABO EL-MAATY A.M., RAGAB R.S.A., SEIDA A.A., 2016 – Assessment of uterine vascular perfusion during the estrous cycle of mares in connection to circulating leptin, and nitric oxide concentrations. *Journal of Equine Veterinary Science* 39, 25-32.
2. ABDELNABY E.A., ABO EL-MAATY A.M., 2017 – Luteal blood flow and growth in correlation to circulating angiogenic hormones after spontaneous ovulation in mares. *Bulgarian Journal of Veterinary Medicine* 20, 97-109.
3. ABDELNABY E.A., ABO EL-MAATY A.M., 2017 – Dynamics of follicular blood flow, antrum growth, and angiogenic mediators in mares from deviation to ovulation. *Journal of Equine Veterinary Science* 55, 51-59.
4. ABO EL-MAATY A.M., ABDELNABY E.A., 2017 – Follicular blood flow, antrum growth and angiogenic mediators in mares from ovulation to deviation. *Animal Reproduction* 14, 1043-1056.
5. ACOSTA T.J., BEG M.A., GINTHER O.J., 2004 – Aberrant blood flow area and plasma gonadotropin concentrations during the development of dominant-sized transitional anovulatory follicles in mares. *Biology of Reproduction* 71, 637-642.
6. ACOSTA T.J., GASTAL E.L., GASTAL M.O., BEG M.A., GINTHER O.J., 2004 – Differential blood flow changes between the future dominant and subordinate follicles precede diameter changes during follicle selection in mares. *Biology of Reproduction* 71, 502-507.

7. ACOSTA T.J., HAYASHI K.G., OHTANI M., MIYAMOTO A., 2003 – Local changes in blood flow within the preovulatory follicle wall and early corpus luteum in the cow. *Reproduction* 125, 759-767.
8. BAILEY C.S., HEITZMAN J.M., BUCHANAN C.N., BARE C.A., SPER R.B., BORST L.B., MACPHERSON M., ARCHIBALD K., WHITACRE M., 2012 – B-mode and Doppler ultrasonography in pony mares with experimentally induced ascending placentitis. *Equine Veterinary Journal* 44, Suppl. 43, 88-94.
9. BAILEY C.S., SPER R.B., SCHEWMAKER J.L., BUCHANAN C.N., BEACHLER T.M., POZOR M.A., WHITACRE M.D., 2012 – Uterine artery blood flow remains unchanged in pregnant mares in response to short-term administration of pentoxifylline. *Theriogenology* 77, 430-436.
10. Baltsen M., Bøgh I.B., Byskov A.G., 2001 – Content of meiosis activating sterols in equine follicular fluids: correlation to follicular size and dominance. *Theriogenology* 56, 133-145.
11. BASHIR S.T., ISHAK G.M., GASTAL M.O., ROSER J.F., GASTAL E.L., 2016 – Changes in intrafollicular concentrations of free IGF-1, activin A, inhibin A, VEGF, estradiol, and prolactin before ovulation in mares. *Theriogenology* 85, 1491-1498.
12. BOAKARI Y.L., FERREIRA J.C., CANESIN H.S., THOMPSON D.L. Jr, LIMA F.S., PANTOJA J.C.F., MEIRA C., 2017 – Influence of two ovulation-inducing agents on the pituitary response and follicle blood flow in mares. *Theriogenology* 100, 95-99.
13. BOLLWEIN H., KOLBERG B., STOLLA R., 2004 – The effect of exogenous estradiol benzoate and altrenogest on uterine and ovarian blood flow during the estrous cycle in mares. *Theriogenology* 61, 1137-1146.
14. BOLLWEIN H., MAYER R., STOLLA R., 2003 – Transrectal Doppler sonography of uterine blood flow during early pregnancy in mares. *Theriogenology* 60, 597-605.
15. BOLLWEIN H., MAYER R., WEBER F., STOLLA R., 2002 – Luteal blood flow during the estrous cycle in mares. *Theriogenology* 57, 2043-2051.
16. BOLLWEIN H., WEBER F., KOLBERG B., STOLLA R., 2002 – Uterine and ovarian blood flow during the estrous cycle in mares. *Theriogenology* 57, 2129-2138.
17. BRITO L.F., BALDRIGHI J.M., WOLF C.A., GINTHER O.J., 2017 – Effect of GnRH and hCG on progesterone concentration and ovarian and luteal blood flow in diestrous mares. *Animal Reproduction Science* 176, 64-69.
18. BROGAN P.T., HENNING H., STOUT T.A., DE RUIJTER-VILLANI M., 2016 – Relationship between colour flow Doppler sonographic assessment of corpus luteum activity and progesterone concentrations in mares after embryo transfer. *Animal Reproduction Science* 166, 22-27.
19. CUERVO-ARANGO J., NEWCOMBE J.R., 2012 – Ultrasound characteristics of experimentally induced luteinized unruptured follicles (LUF) and naturally occurring hemorrhagic anovulatory follicles (HAF) in the mare. *Theriogenology* 77 514-524.
20. DONADEU F.X., GINTHER O.J., 2002 – Follicular waves and circulating concentrations of gonadotrophins, inhibin, and estradiol during the anovulatory season in mares. *Reproduction* 124, 875-885.
21. DONADEU F.X., GINTHER O.J., 2004 – Interrelationships of estradiol, inhibin, and gonadotropins during follicle deviation in pony mares. *Theriogenology* 61, 1395-1405.
22. ESTELLER-VICO A., LIU I.K., VAUGHAN B., STEFFEY E.P., BROSNAN R.J., 2015 – Effects of vascular elastosis on uterine blood flow and perfusion in anesthetized mares. *Theriogenology* 83, 988-994.

23. FERREIRA J.C., CANESIN H.S., IGNÁCIO F.S., ROCHA N.S., PINTO C.R., MEIRA C., 2015 – Effect of age and endometrial degenerative changes on uterine blood flow during early gestation in mares. *Theriogenology* 84, 1123-1130.
24. FERREIRA J.C., FILHO L.F.N., BOAKARI Y.L., CANESIN H.S., THOMPSON D.L. JR, LIMA F.S., MEIRA C., 2018 – Hemodynamics of the corpus luteum in mares during experimentally impaired luteogenesis and partial luteolysis. *Theriogenology* 107, 78-84.
25. FERREIRA J.C., GASTAL E.L., GINTHER O.J., 2008 – Uterine blood flow and perfusion in mares with uterine cysts: effect of the size of the cystic area and age. *Reproduction* 135, 541-550.
26. FERREIRA J.C., IGNÁCIO F.S., ROCHA N.S., THOMPSON D.L. JR, PINTO C.R., MEIRA C., 2015 – Real-time characterization of the uterine blood flow in mares before and after artificial insemination. *Animal Reproduction Science* 160, 90-96.
27. FRASER H.M., DUNCAN W.C., 2009 – Regulation and manipulation of angiogenesis in the ovary and endometrium. *Reproduction Fertility and Development* 21, 377-392.
28. GASTAL M.O., GASTAL E.L., BEG M.A., GINTHER O.J., 2010 – Short-term feed restriction decreases the systemic and intrafollicular concentrations of leptin and increases the vascularity of the preovulatory follicle in mares. *Theriogenology* 73, 1202-1209.
29. GHARAGOZLOU F., AKBARINEJAD V., YOUSSEFI R., MASOUDIFARD M., HASANI N., 2014 – Reduced anti-Müllerian hormone (AMH) in mares with hemorrhagic anovulatory follicles. *Iranian Journal Veterinary Research* 15, 336-340.
30. GINTHER O.J., 1990 – Folliculogenesis during the transitional period and early ovulatory season in mares. *Journal Reproduction and Fertility* 90, 311-320.
31. GINTHER O.J., BEG M.A., DONADEU F.X., BERGFELT D.R., 2003 – Mechanism of follicle deviation in monovular farm species. *Animal Reproduction Science* 78, 239-257.
32. GINTHER O.J., GASTAL E.L., GASTAL M.O., BEG M.A., 2006 – Conversion of, a viable preovulatory follicle into a hemorrhagic anovulatory follicle in mares. *Animal Reproduction* 3, 29-40.
33. GINTHER O.J., GASTAL E.L., GASTAL M.O., BEG M.A., 2007 – Incidence, endocrinology, vascularity, and morphology of hemorrhagic anovulatory follicles in mares. *Journal of Equine Veterinary Science* 27, 130-139.
34. GINTHER O.J., GASTAL E.L., GASTAL M.O., BERGFELT D.R., BAERWALD A.R., PIERSON R.A., 2004 – Comparative study of the dynamics of follicular waves in mares and women. *Biology of Reproduction* 71, 1195-1201.
35. GINTHER O.J., GASTAL E.L., GASTAL M.O., SIDDIQUI M.A., BEG M.A., 2007 – Relationships of follicle versus oocyte maturity to ultrasound morphology, blood flow, and hormone concentrations of the preovulatory follicle in mares. *Biology of Reproduction* 77, 202-208.
36. ISHAK G.M., BASHIR S.T., GASTAL M.O., GASTAL E.L., 2017 – Pre-ovulatory follicle affects corpus luteum diameter, blood flow, and progesterone production in mares. *Animal Reproduction Science* 187, 1-12.
37. JIANG J.Y., MACCHIARELLI G., TSANG B.K., SATO E., 2003 – Capillary angiogenesis and degeneration in bovine ovarian antral follicles. *Reproduction* 125, 211-223.
38. LEMES K.M., SILVA L.A., ALONSO M.A., CELEGHINI E.C.C., PUGLIESI G., CARVALHO H.F., AFFONSO F.J., SILVA D.F., LEITE T.G., DE ARRUDA R.P., 2017 – Follicular dynamics, ovarian vascularity and luteal development in mares with early or late postpartum ovulation. *Theriogenology* 1, 96, 23-30.

39. OUSEY J.C., KÖLLING M., NEWTON R., WRIGHT M., ALLEN W.R., 2012 – Uterine haemodynamics in young and aged pregnant mares measured using Doppler ultrasonography. *Equine Veterinary Journal* 44, Suppl. 41, 15-21.
40. SPSS, 2007 – Statistical Package for Social Sciences, SPSS Inc., Chicago, IL, USA Copyright©for Windows, version 16.0.
41. TODA T., 1990 – Ultrasonographical study on luteinized unruptured follicle. *Nippon Sanka Fujinka Gakkai Zasshi* 42, 1195-1202.
42. VARUGHESE E.E., BRAR P.S., HONPARKHE M., GHUMAN S.P., 2014 – Correlation of blood flow of the preovulatory follicle to its diameter and endocrine profile in dairy buffalo. *Reproduction in Domestic Animals* 49, 140-144.
43. WATSON E.D., AL-ZI'ABI M.O., 2002 – Characterization of morphology and angiogenesis in follicles of mares during spring transition and the breeding season *Reproduction* 124, 227-234.